

## Survey of OH Masers at 1665 MHz. III\* Galactic Longitudes 233° to 326°

*J. L. Caswell and R. F. Haynes*

Division of Radiophysics, CSIRO,  
P.O. Box 76, Epping, N.S.W. 2121.

### *Abstract*

We have searched the galactic plane from longitude 233° to 326° for OH emission on the 1665 MHz transition. Between longitudes 270° and 326°, where the survey zone was a uniformly sampled grid, we detected 35 OH maser sources, including 24 new ones; most are of the Type I variety that delineates sites of current star formation, and many of the sites are young, with no well-developed HII regions in the vicinity. By combining the present results with those of earlier surveys (longitudes 326° → 360° → 2°: Parts I and II) we have improved on previous estimates of the galactic distribution of these masers.

All sources were studied in both circular polarisations on the 1665 and 1667 MHz transitions of the OH ground state; measurements of the 1612 and 1720 MHz transitions will be needed to single out any masers of different varieties, such as those associated with late-type stars rather than regions of star formation.

Three individually interesting discoveries are: OH 301.14-0.23, which shows weak 'high-velocity' emission displaced more than 20 km s<sup>-1</sup> from the main features, similar to the displacements seen in the associated H<sub>2</sub>O maser; OH 310.06-3.02, which is probably an unusual variety of late-type star; and OH 311.64-0.38, whose systemic velocity of +34 km s<sup>-1</sup> indicates a location outside the solar circle, in a previously uncharted extension of the Carina spiral arm, 16.3 kpc from the Sun.

### 1. Introduction

The present search for main-line OH masers in the galactic plane was conducted in the same manner as our previous surveys (longitudes 326°-340°: Caswell *et al.* 1980, hereafter Part I; longitudes 340°-360°-2°: Caswell and Haynes 1983; hereafter Part II). The objective was to increase the galactic longitude coverage in order to provide a more complete catalogue and to better estimate the spatial density of Type I OH masers (associated with star-formation regions) at quite large distances (~10 kpc) from the galactic centre.

Observations were made with a dual-channel 18 cm parametric amplifier receiver installed on the Parkes 64-m paraboloid. For each circular polarisation 512-point spectra were obtained simultaneously. The system temperature was ~75 K on cold regions of sky. The intensity calibration is relative to Hydra A, for which a total flux density of 36 Jy was assumed (i.e. 18 Jy in each sense of circular polarisation; the ratio of flux density to antenna temperature for *each* polarisation is 0.8 Jy K<sup>-1</sup>). The beamwidth to half-power is 12' arc at 1665 MHz.

\* Part II, *Aust. J. Phys.*, 1983, 36, 361-99.

*(a) The Search: 1981 September 16–21*

Observations were made on the 1665 MHz transition (adopted rest frequency 1665.402 MHz) covering a grid at  $b = 0^\circ$  and  $\pm 0^\circ.2$  and spaced  $0^\circ.2$  in longitude from  $300^\circ$  to  $326^\circ$ . Positions with  $|b| \geq 0^\circ.4$  were observed where OH emission was detected at the edge of the original grid or where the continuum emission (see Haynes *et al.* 1978) extends significantly outside latitudes  $\pm 0^\circ.3$  (including a search at the positions of discrete HII regions displaced from the galactic plane).

The spectrum bandwidth analysed was 1 MHz; the corresponding radial velocity range (relative to the local standard of rest) was  $-90$  to  $+90$  km s $^{-1}$  for  $l < 320^\circ$ , and  $-110$  to  $+70$  km s $^{-1}$  for  $320^\circ < l < 326^\circ$ . The resolution, after Hanning weighting, was 4 kHz ( $\equiv 0.7$  km s $^{-1}$ ). At each grid point a 5-minute integration was made; combined with a 15-minute reference, this yielded an r.m.s. noise level of  $\sim 0.1$  K ( $\equiv 0.08$  Jy) in each sense of polarisation. In several earlier sessions longitudes  $270^\circ$ – $300^\circ$  were searched at  $b = 0^\circ$ ; the positions of discrete continuum sources with  $l$  between  $233^\circ$  and  $300^\circ$  were also studied.

*(b) Further OH Study: 1982 February 8–13*

A more accurate position for each OH maser was derived from spectra taken on a grid with 6' arc spacing centred at the approximate source position. Spectra with higher frequency resolution ( $0.8$  kHz  $\equiv 0.14$  km s $^{-1}$  covering a total bandwidth of  $0.2$  MHz) were then obtained at the source position. Finally, observations were made on the 1667 MHz transition (adopted rest frequency 1667.359 MHz).

*(c) Complementary H<sub>2</sub>O Study: 1981 December and 1982 April*

In these observations of the  $6_{16}-5_{23}$  transition of H<sub>2</sub>O at 22.23508 GHz we searched for H<sub>2</sub>O masers associated with the new OH masers. The H<sub>2</sub>O maser detections are summarised here and details will be given elsewhere (Caswell *et al.* 1987; hereafter CBFW 87).

**2. Results***(a) OH Emission: Tabulation and Figures*

Table 1 lists the main-line emission sources detected in the survey. Several of these had been discovered in earlier searches at the positions of strong HII regions. Details of the sources are best displayed in the line profiles (see Figs 1–11), with Table 1 providing a convenient summary. Note that the rest frequencies adopted in earlier Parkes observations were smaller by 1 kHz, and that for precise comparisons with the present data the corresponding velocity shift (of  $0.18$  km s $^{-1}$ ) must be allowed for. Positions of most of the previously known sources have been remeasured and a weighted average position is quoted. Earlier position measurements were usually only of the polarisation showing strongest emission whereas current measurements study all features simultaneously, limited only by the signal-to-noise ratio for weak features. Except where otherwise stated, positions of all features seen in the profiles are coincident to within the uncertainties.

The radial velocity range quoted in column 5 refers to the total velocity extent seen in either transition. The peak intensities observed in each transition are listed in columns 6, 7, 8 and 9, with the sense of circular polarisation that exhibits the strongest emission indicated by L or R. In all cases the positioning measurements

Table 1. OH main-line masers in galactic plane between longitudes 270° and 326°

(1) Galactic coordinates l b	(2) Position (1950)		(3) Dec. ° ' "	(4) rms error " "	(5) Radial velocity <sup>A</sup> (km s <sup>-1</sup> )	(6) Intensity (and polarization) of peak <sup>B</sup>			(8) 1612 (Jy)	(9) 1720 (Jy)	(10) Fig. Nos. and OH refs <sup>C</sup>	(11) H <sub>2</sub> O refs.	(12) Radio continuum	(13) Kinematic distance (kpc)
	R.A. h m s	° ' "				1665 (Jy)	1667 (Jy)	1672 (Jy)						
285.26+0.05	10 29 37.2	-57 46 46	12		+2,+14	26(L)	0.6(R)	<2	<2	Fig. 1; RCG;MRG	B+80; P81	Strong HII	5.0	
291.57+0.43	11 12 54.1	-60 53 08	20		+14,+15	[8.5(R)]	<2	<1.5	<1.5	RCG;MRG	B+80; P81	HII	8.5	
291.61+0.53	11 12 51.4	-60 59 43	19		+17,+20	7.6(L)	1.1(L)	<3	<3	Fig. 1 (MRG)	P81	Compact HII	8.5	
297.66+0.98	12 01 33.7	-63 05 11	12		+23,+29	3.6(L)	0.8(L)			Fig. 1	B+80	HII	11.7	
299.02+0.13	12 14 44.0	-62 12 28	32		+20,+25	1.2(L)	<0.4			Fig. 2	BS; P81	HII	11.8	
300.51+0.18	12 27 14.4	-62 40 26	~60?		+22,+23	0.6(R)	<0.3			Fig. 2	P 81		12.5	
300.97+0.15	12 32 02.2	-61 22 56	12		-42,-34	14.2(R)	4.2(L)	<1	<1	Fig. 2; RCG	B+80; P81	HII	5.1	
301.14+0.23	12 32 42.5	-62 46 02	16		-64,-34E	34(L)	6(R)			Fig. 3	BS; P81	Weak source	5.2	
305.20+0.21	13 07 55.0	-62 18 41	15		-41,-37	9.8(R)	<0.5			Fig. 4; CHG	B+80	Strong HII	(3.4); 8.1	
305.21+0.03	13 08 07.8	-62 29 29	18		-35,-33	6.8(L)	<0.5			Fig. 4	P82	Strong HII	(3.5); 8.0	
305.36+0.15	13 09 22.7	-62 21 15	16		-43,-30	38(R)	8.3(R)	<2	<2	Fig. 4; GMR;RCG	B+80	Strong HII	(3.2); 8.3	
305.81+0.24	13 13 30.6	-62 42 28	18		-37,-34	3.8(R)	1.0(R)			Fig. 2	P81	Edge of HII	2.4; 9.3	
306.32+0.36	13 18 02.9	-62 46 27	~60?		-24,-22	[~2(L)]		<1	<1	Fig. 5; RCG	BS; P81	Compact HII	(1.2); 10.7	
308.92+0.12	13 39 37.0	-61 53 44	17		-56,-50	62(R)	13.2(L)			Fig. 5	P82	Compact HII	4.8; 7.7	
309.39+0.13	13 43 57.5	-62 03 08	28		-54,-49	1.8(R)	<0.4			Fig. 6		Weak, extended	4.5; 8.2	
309.92+0.48	13 47 12.5	-61 19 58	16		-64,-58	37(L)	3.6(L)	<1	<1	Fig. 5; RCG	K, P82	Extension of HII	6.4	
310.06+3.02	13 55 46.4	-64 42 22	18		-13,-8	1.4(R)	0.6(R)			Fig. 6	P81	Not mapped	0.2; (12.7)	
311.64+0.38	14 03 00.9	-61 43 54	12		+28,+40	8.1(R)	11.1(L)	5		Fig. 6	P81	Weak	16.3	
311.94+0.14	14 04 11.2	-61 09 07	[H,0]		-42,-40	0.5(L)	<0.5			Fig. 7	BS; P81	Near compact HII	(3.7); 9.7	
312.60+0.05	14 09 36.3	-61 02 41	12		-70,-58	12.8(R)	0.9(R)			Fig. 7	P81	Weak, extended	5.8; 7.7	
313.47+0.19	14 16 01.7	-60 38 10	24		-11,-5	2.5(L)	<0.2			Fig. 7	P82	Compact HII	(0.3); 13.4	
316.40+0.30	14 39 27.1	-60 30 22	36		-9,-2	0.6(R)	<0.3			Fig. 7	P82	Compact HII	14.7	
316.64+0.08	14 40 30.0	-59 42 18	30		-28,-15	2.6(L)	2.0(R)			Fig. 8; CHG	P82	Near strong HII	1.5; (13.1)	
316.76+0.02	14 41 09.4	-59 35 45	28		-44,-37	1.9(R)	<0.5			(H,C)	B+80	Strong HII	2.5; (12.1)	
316.81+0.07	14 41 38.9	-59 37 11	20		-44,-37	3.2(L)	<0.5			Fig. 8	B+80	Strong HII	2.5; (12.1)	
318.05+0.08	14 49 54.7	-58 56 41	15		-54,-51	57(R)	1.4(R)			Fig. 8	P81	Weak, extended	3.7; (11.1)	
318.95+0.20	14 57 06.3	-58 46 47	16		-42,-30	1.2(R)	1.3(R)			Fig. 9	P81	Compact HII	2.0; 13.1	
319.39+0.02	14 59 22.6	-58 25 00	22		-11,-7	1.5(R)	2.0(L)			Fig. 9	P81	Extended HII	(0.9); 14.2	
319.83+0.21	15 03 04.3	-58 22 10	29		-22,-6	1.4(L)	0.8(L)			Fig. 10	P81	Very weak	0.9; 14.3	
320.23+0.28	15 05 59.3	-58 14 03	12		-69,-59	20.5(R)	6.1(L)	<1	<1	Fig. 9; RCG	SB; P82	Compact HII	5.0; 10.4	
321.14+0.53	15 12 51.9	-57 58 58	34		-73,-60	2.1(R)	0.5(L)			Fig. 10	P82	HII	4.5; (11.0)	
322.16+0.23	15 14 46.8	-56 27 34	24		-62,-60	2.9(R)	0.7(R)			Fig. 10	BS; P81	Strong HII	3.6; (12.2)	
323.46+0.08	15 25 28.0	-56 20 48	15		-73,-64	10.6(R)	5.7(L)			Fig. 10	P81	Weak source	4.8; 11.2	
324.20+0.12	15 29 01.8	-55 45 11	15		-94,-81	14(L)	0.5(L)	<1	<1	Fig. 11; RCG	B+80	Compact HII	8.1	
324.70+0.33	15 31 04.5	-55 48 25	42		-56,-49	1.5(R)	0.5(L)			Fig. 11	P82	Nothing?	3.6; 12.7	

A. Range of radial velocity over which emission is detectable.

B. Intensities at 1665 and 1667 MHz are for epoch 1982 February, except when in parentheses.

C. RCG, Robinson et al. (1974); MRG, Manchester et al. (1970); CHG, Caswell et al. (1977); GMR, Goss et al. (1970); HCC, Haynes et al. (1976); B+80, Batchelor et al. (1980); P81 & P82, unpublished Parkes observations in 1981 & 1982 to be published (Caswell et al. 1987); BS, Braz and Scalise (1982); K, Kaufmann et al. (1977); SB, Scalise and Braz (1980).

D. Near and Far distances are given; the less likely value is enclosed in parentheses.

E. Note wide velocity range - see text, 2(b).

F. Rapidly variable - see text, 2(b)

were made at 1665 MHz. The intensities are for 1982 February, except where they are given in parentheses; measurements at other epochs are usually taken from the reference of column 10, and discussed in the notes of the following subsection. Associated H<sub>2</sub>O masers have been found in the direction of most of the OH sources, and a reference is given in column 11. The radio continuum emission in each direction, as seen at 5 GHz with 4' arc beam (Haynes *et al.* 1978) is summarised in column 12. The kinematic distance of column 13 is based on the Schmidt (1965) rotation model, modified by the adoption of constant rotational velocity of 250 km s<sup>-1</sup> outside the solar circle (assumed to be 10 kpc from the galactic centre); both near and far distances are quoted, with the less likely one enclosed in parentheses. Where a maser is clearly associated with an HII region whose velocity has been reliably measured (Caswell and Haynes 1986), the HII velocity has been preferred to the mean OH velocity for the kinematic distance estimate.

(b) *Notes on Some Individual OH Masers*

Here we draw attention to any unusual properties and make comparisons with data from earlier epochs in the case of sources known for several years.

*OH 285.26–0.05 (Fig. 1).* Well-known (Manchester *et al.* 1970; Robinson *et al.* 1974). The 1982 spectrum at 1665 MHz generally resembles that of 1970, with the RH feature at  $v = +4.1$  km s<sup>-1</sup> and the LH feature at  $v = +5.8$  km s<sup>-1</sup> now being 1.5 times stronger. The LH feature at  $v = +5.2$  km s<sup>-1</sup> increased from 6 Jy in 1970 to 43 Jy in March 1976, and despite a subsequent decline to 26 Jy (1982) it remains the strongest feature. The associated radio HII region is not prominent optically, and its distance is estimated as  $\sim 5$  kpc by Goss *et al.* (1972) using HI absorption measurements. IR data at 10 and 20  $\mu$ m (Frogel and Persson 1974) show a central component with extended wings.

*OH 291.57–0.43 (no figure).* First detected by Manchester *et al.* (1970) but *not currently detectable* (1982). In 1970 the RH feature at  $v = +15.6$  km s<sup>-1</sup> had a peak intensity of 8.5 Jy, and we measured a similar value in July 1976; weak features, 2.2 Jy (LH) at  $v = +13.2$  and 3.4 Jy (RH) at  $v = +16.3$ , were also present in 1976 but have now vanished. (Note that the LH feature at  $v = +18.1$  km s<sup>-1</sup> seen in the Manchester *et al.* profile is from another source, OH 291.61–0.53–q.v.) The H<sub>2</sub>O maser at this position is still (December 1981) very strong.

*OH 291.61–0.53 (Fig. 1).* The position of this new source was first determined in the present observations, but with hindsight we see that this source was responsible for the weak LH feature at  $v = +18.1$  km s<sup>-1</sup> seen in the Manchester *et al.* (1970) observations at 291.57–0.43; i.e. it was near the half-power point with the beam centred 6' arc off source. The intensity of this feature has remained remarkably constant for more than a decade (including our unpublished measurements in 1976). The weak 1667 MHz emission near  $v = +19$  km s<sup>-1</sup> seems to be from this position rather than from 291.57–0.43 (an inference drawn from comparing spectra at just

---

**Figs 1–11.** Spectra of OH main-line masers. The continuous thick curve denotes the right-hand sense of circular polarisation and the thin (dashed) curve denotes the left-hand sense. In all figures the intensity scale refers to one sense of polarisation, so that the total intensity is the sum (not the mean) of the intensities in each polarisation. The velocity resolution is 0.14 km s<sup>-1</sup> (0.8 kHz). The profiles were observed in February 1982.

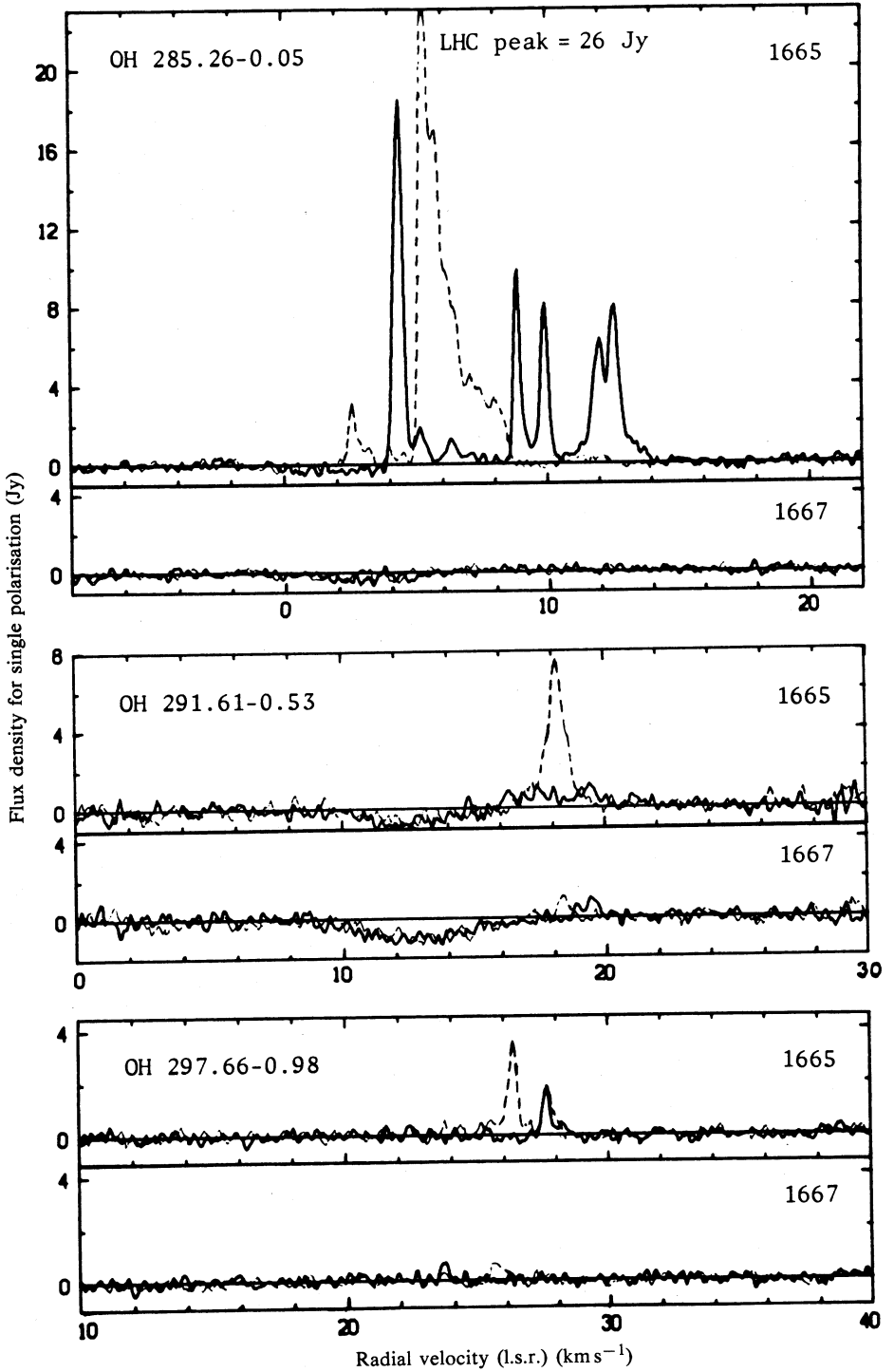


Fig. 1

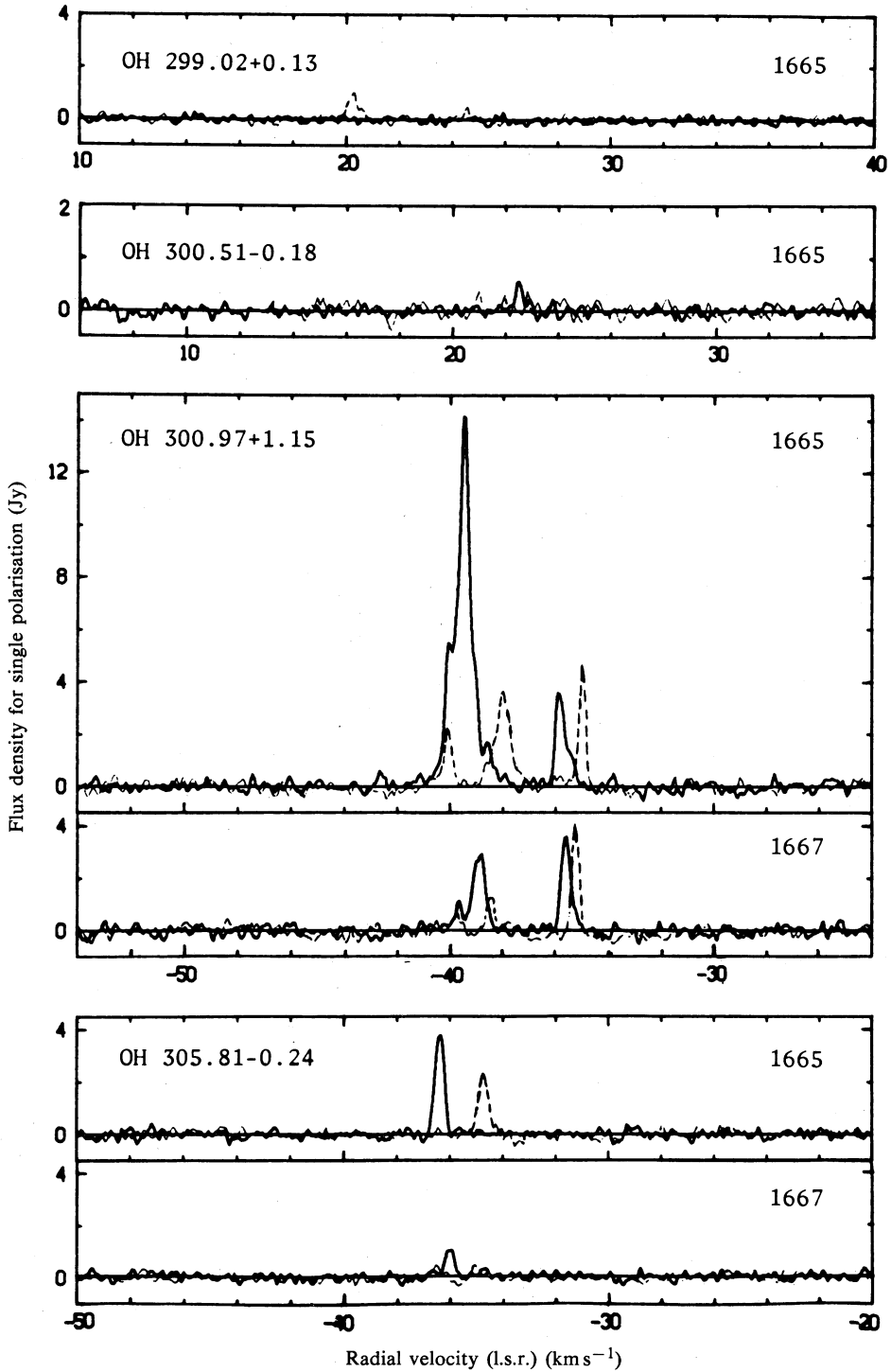


Fig. 2

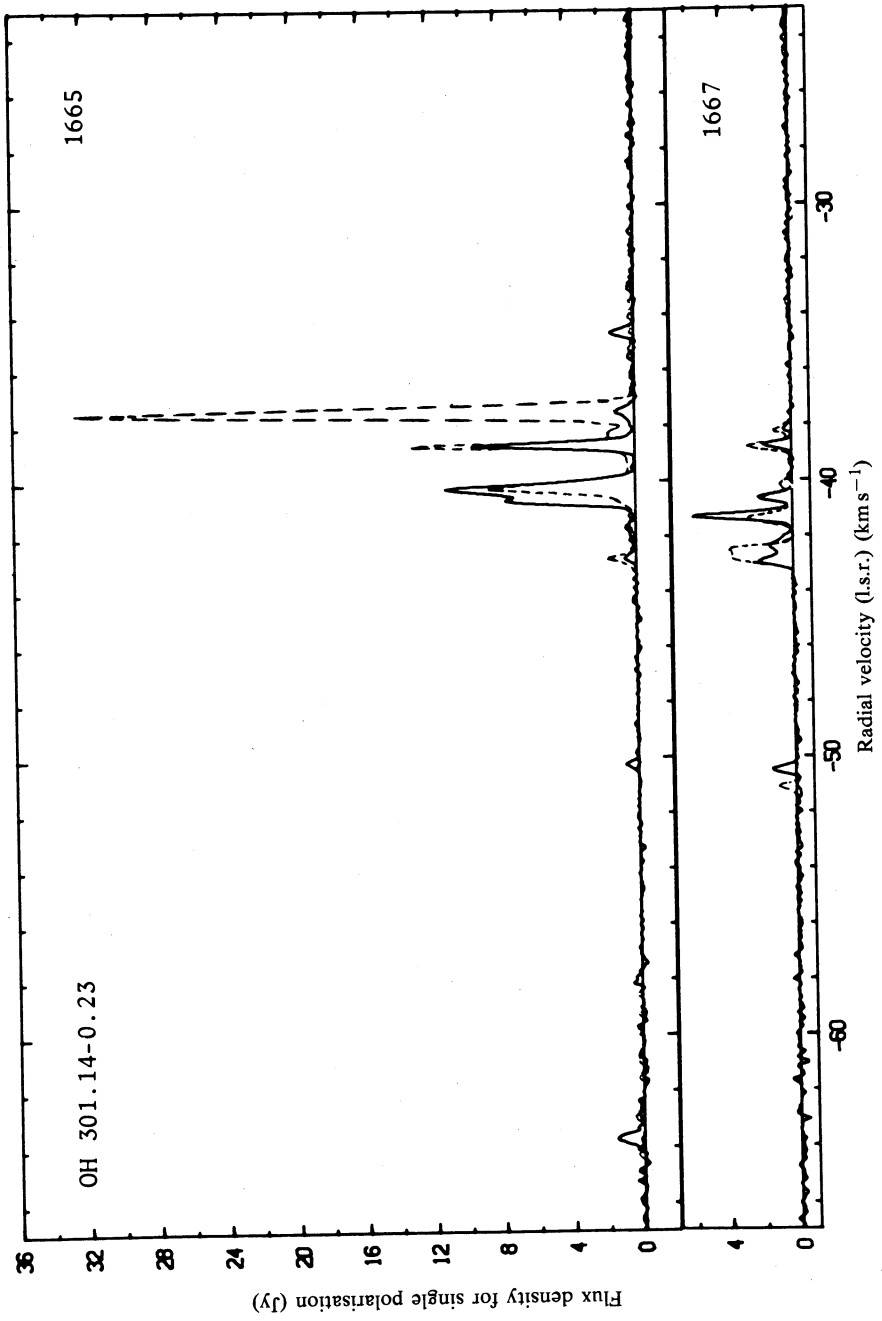


Fig. 3

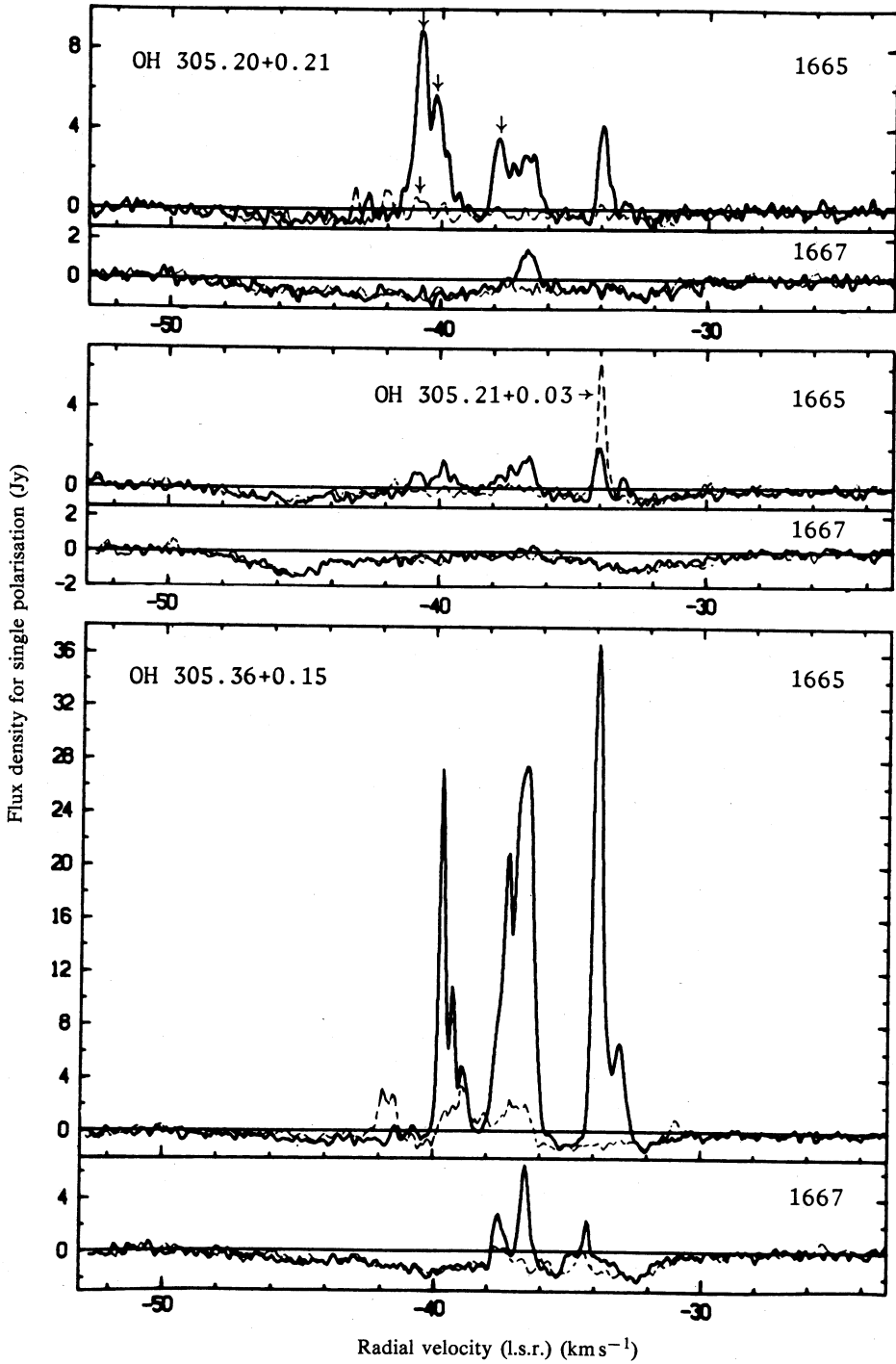


Fig. 4

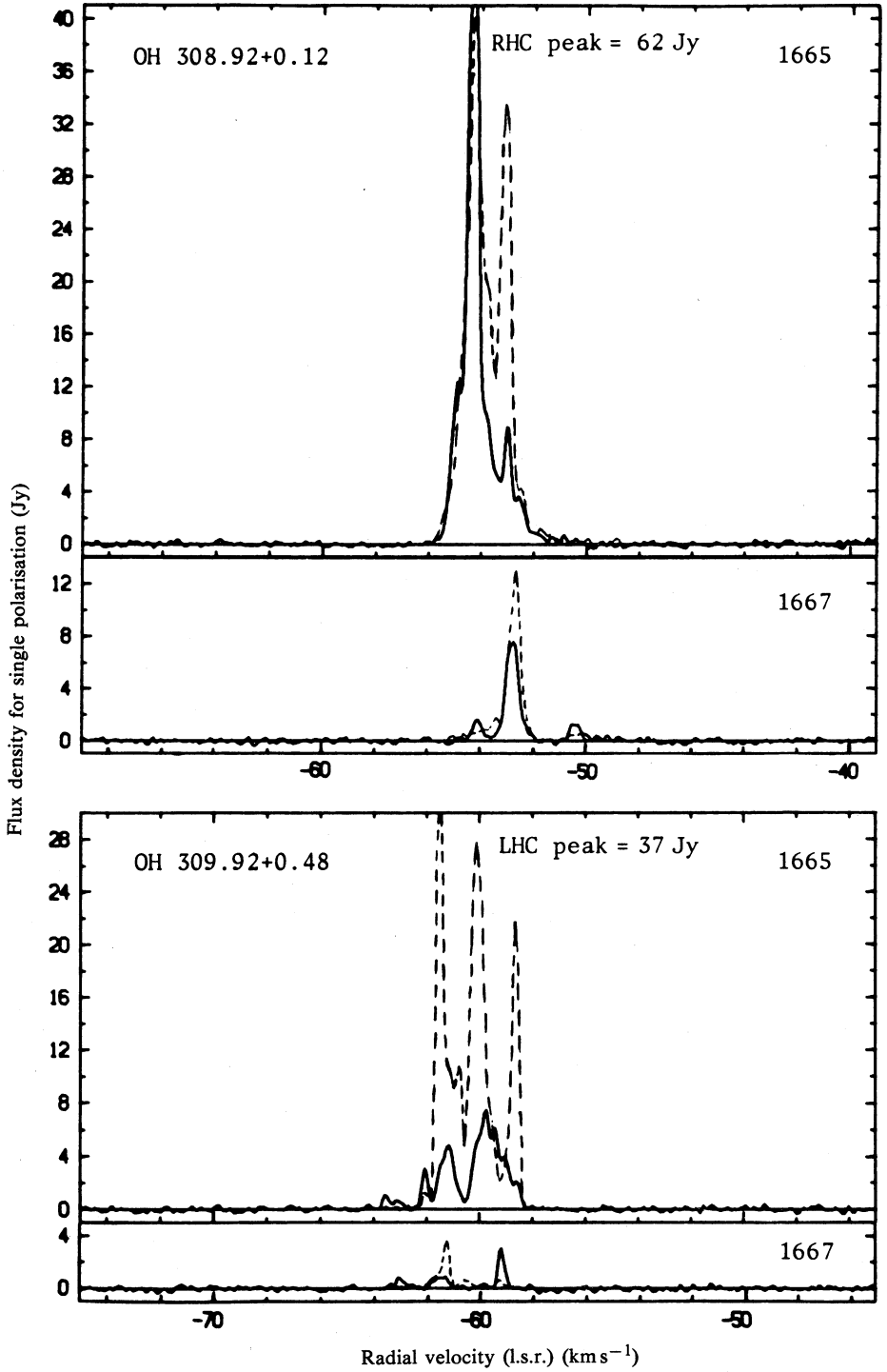


Fig. 5

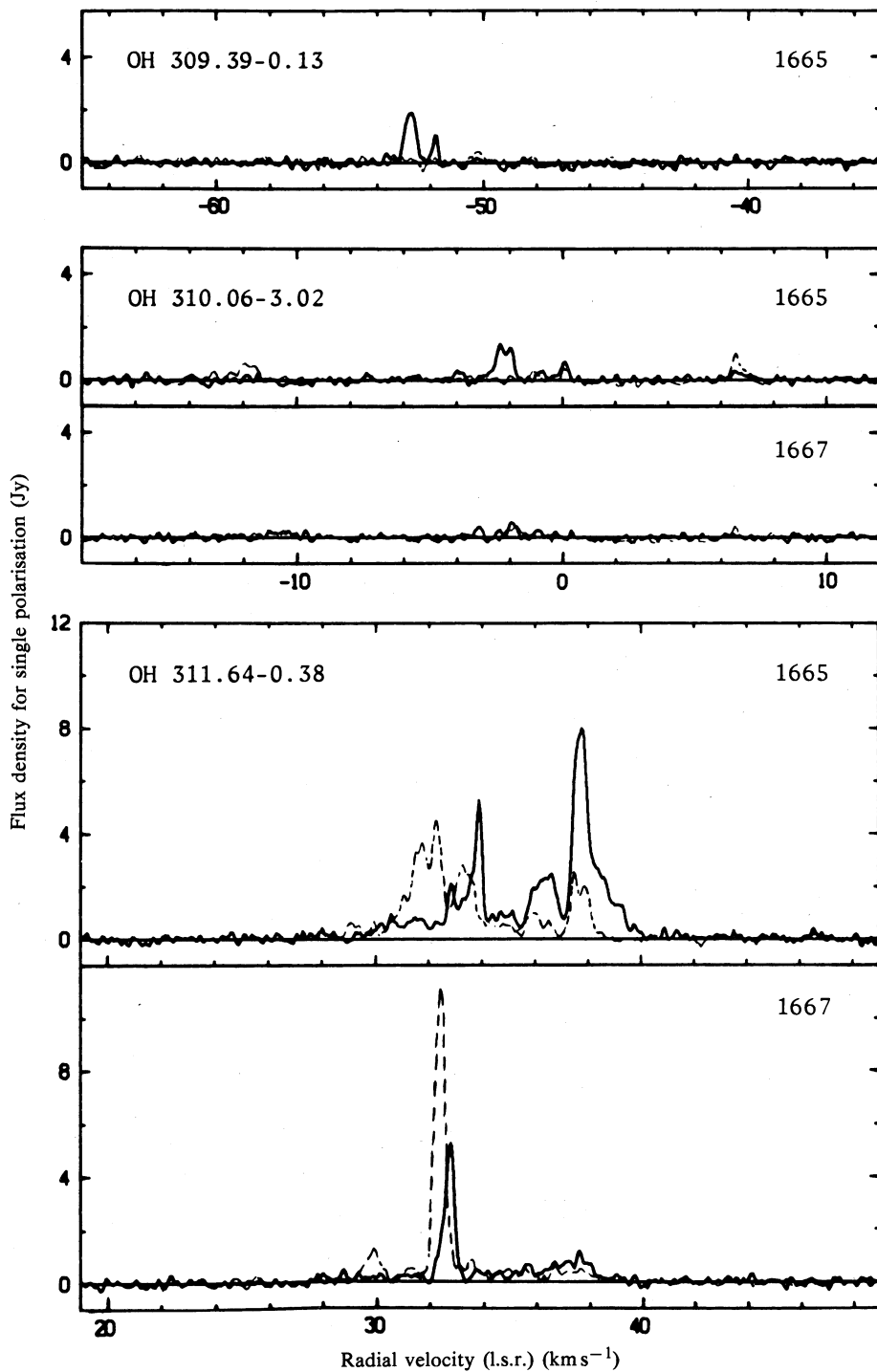


Fig. 6

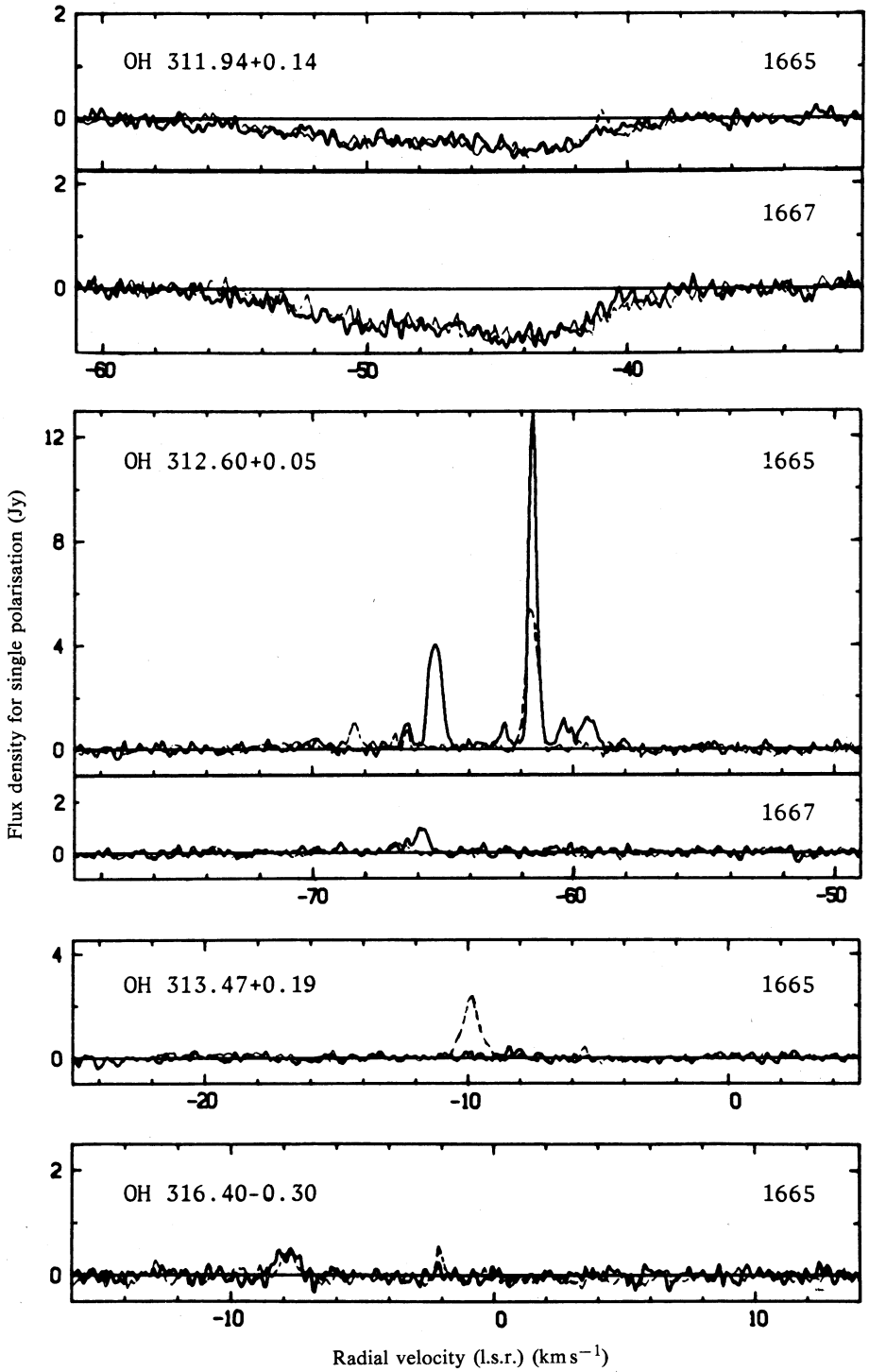


Fig. 7

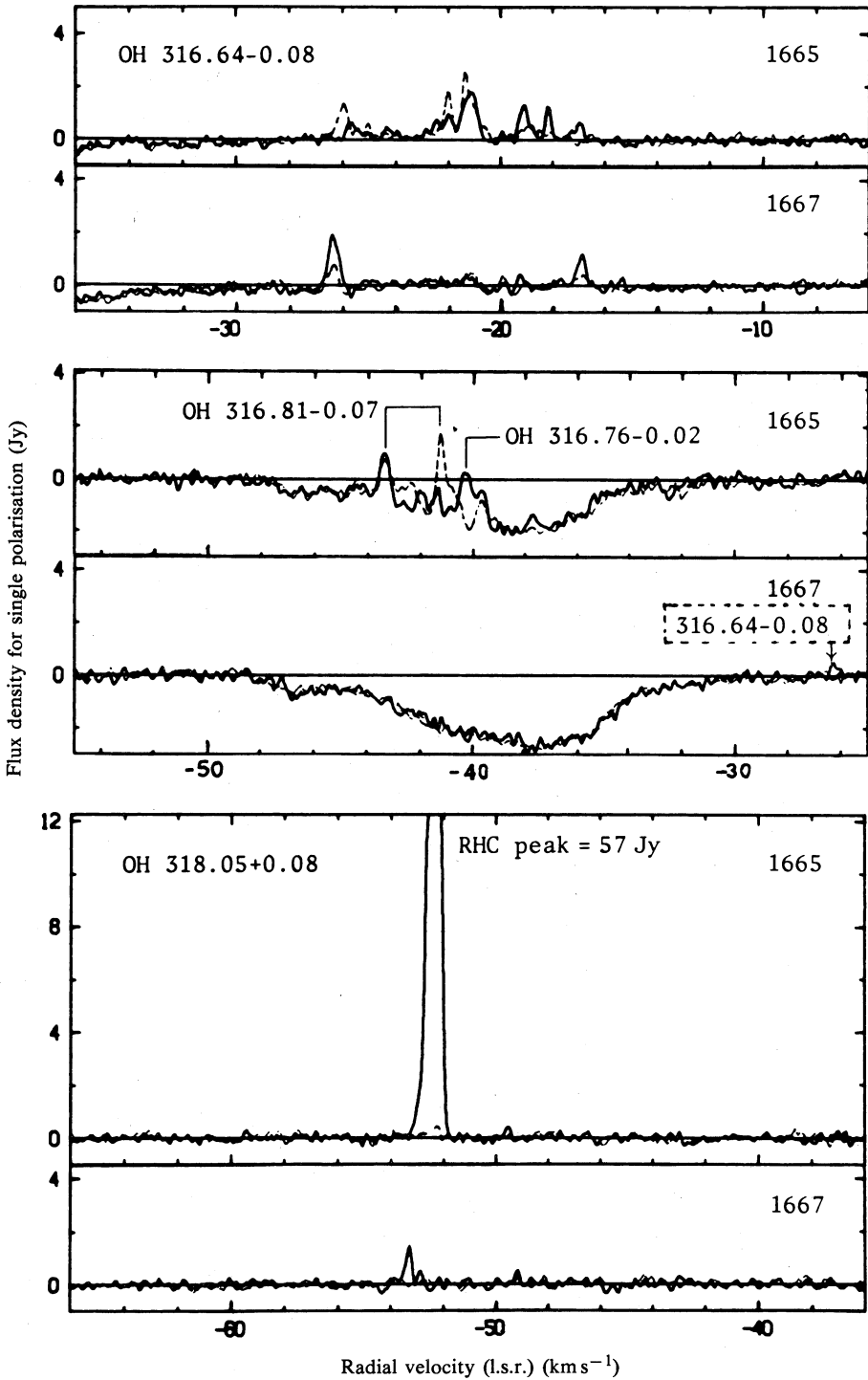


Fig. 8

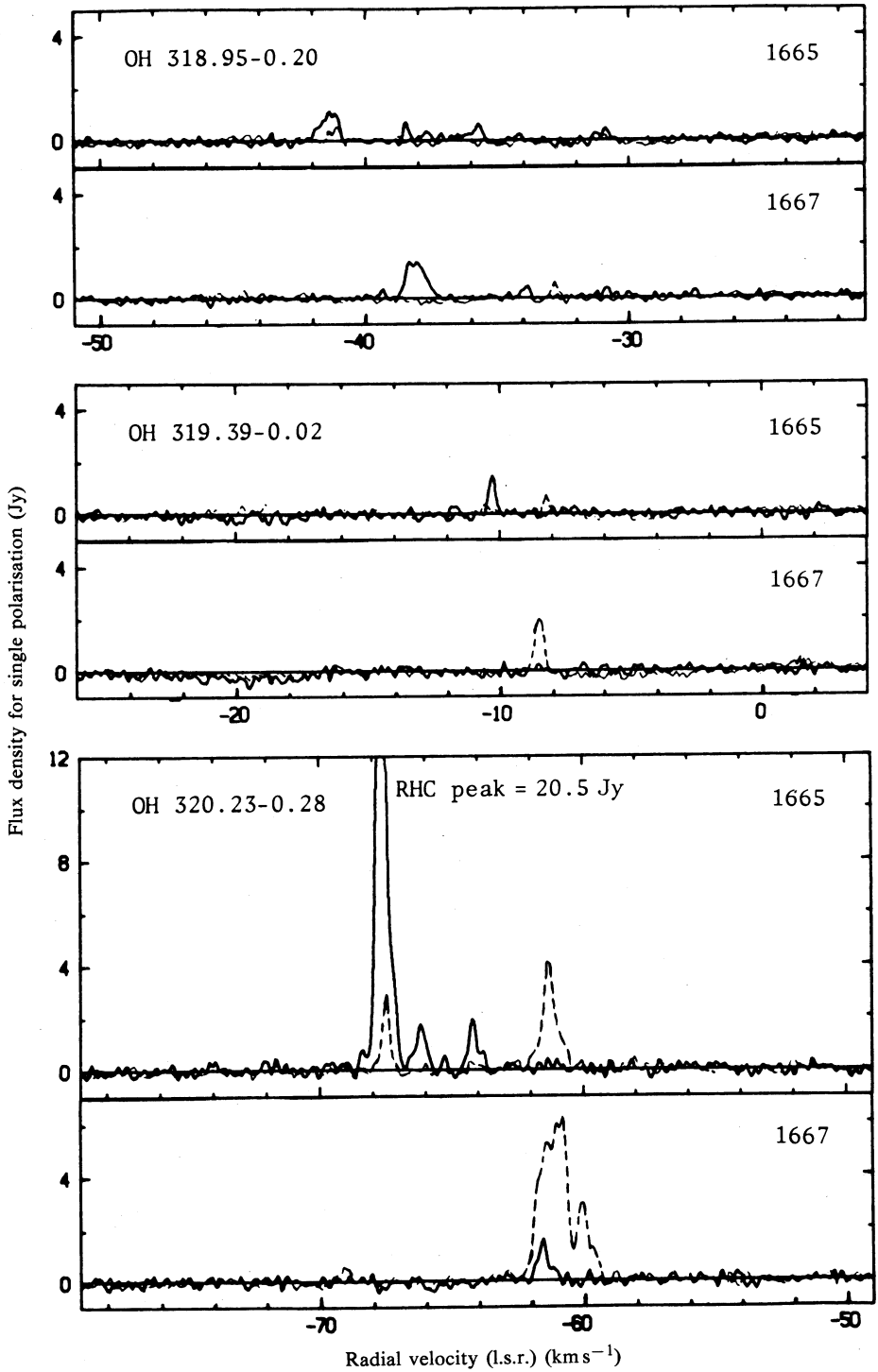


Fig. 9

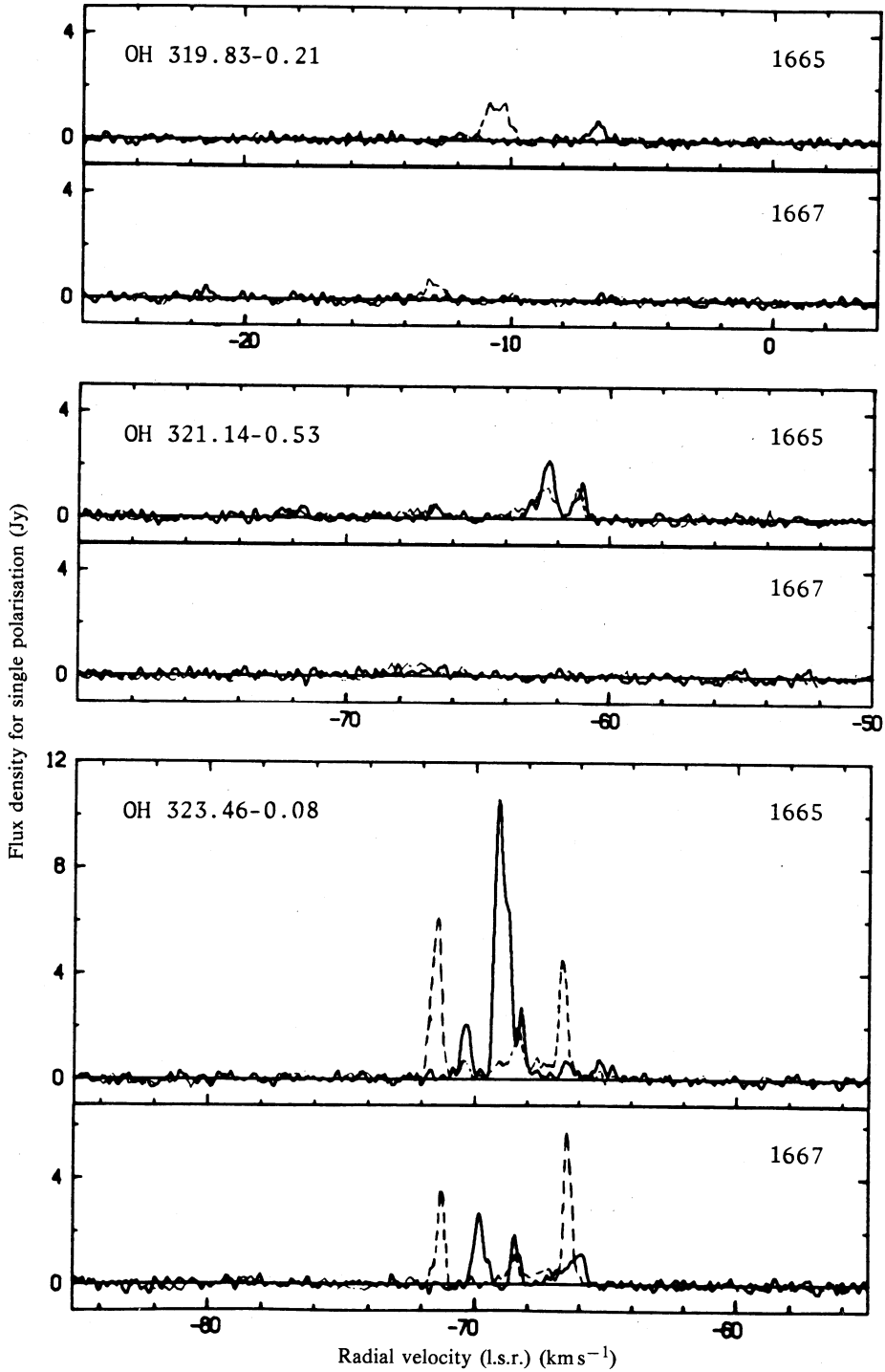


Fig. 10

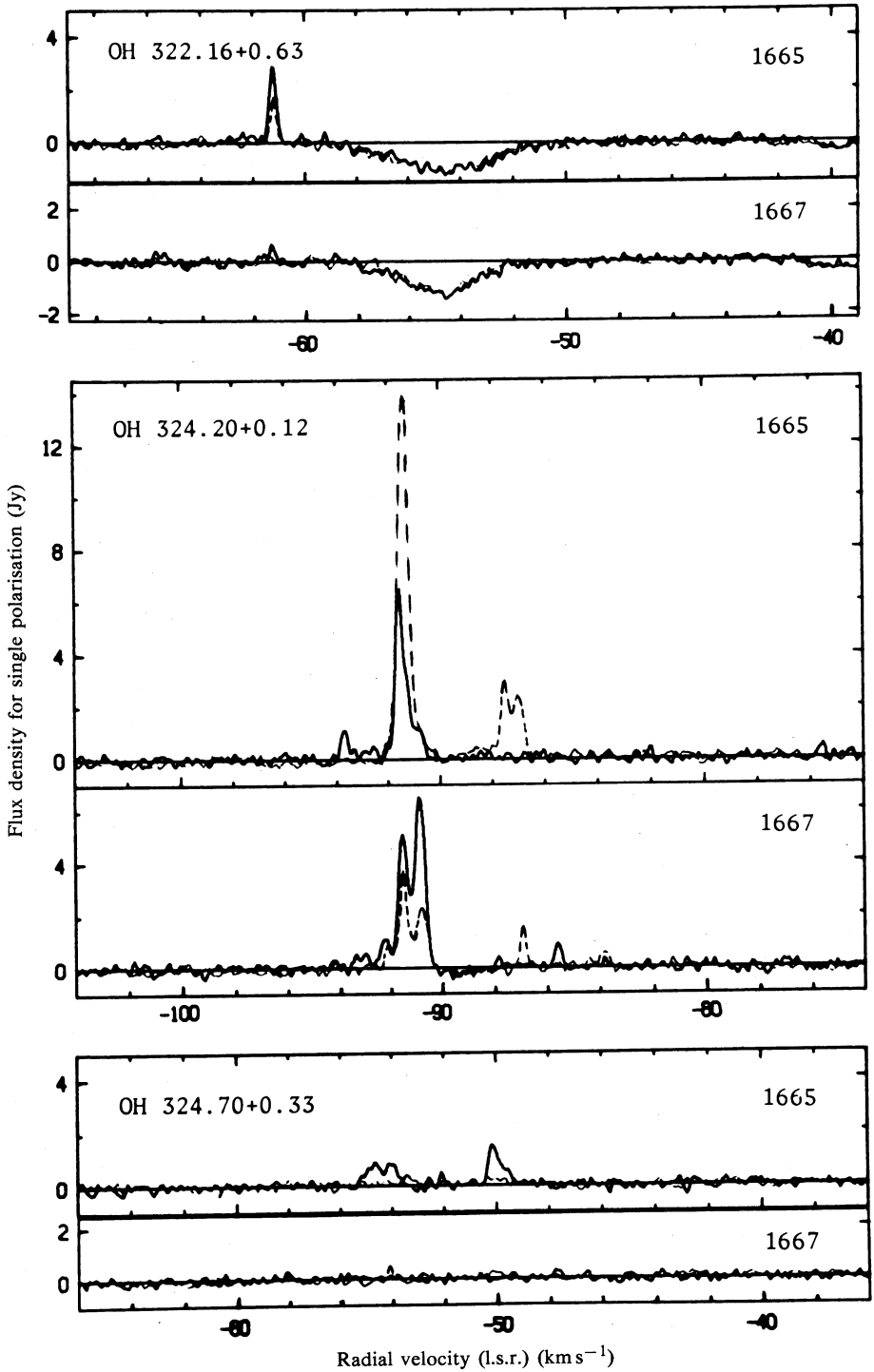


Fig. 11

these two positions); an  $\text{H}_2\text{O}$  maser coincides with OH 291.61–0.53, and three other  $\text{H}_2\text{O}$  masers lie within 6' arc. The associated HII region is one of the most luminous in the Galaxy and several components are seen in the high resolution observations of Retallack and Goss (1980). IR data were discussed by Frogel *et al.* (1977).

OH 299.02+0.13 (Fig. 2). A new source, associated with a compact HII region and an  $\text{H}_2\text{O}$  maser. An extended radio supernova remnant, probably unrelated, is also seen in this direction.

OH 300.97+1.15 (Fig. 2). Discovered by Robinson *et al.* (1974); all features of the 1665 MHz OH maser have shown very little variation (<20%) over the past decade. The 1667 MHz spectrum of Robinson *et al.* probably has a velocity error in the RH polarisation, such that the feature shown at velocity  $-37.5 \text{ km s}^{-1}$  is actually at  $v = -35.8 \text{ km s}^{-1}$ ; with this correction the 1667 MHz spectrum is also seen to have undergone no significant variation. Oppositely polarised pairs of features in the velocity range  $-31$  to  $-32 \text{ km s}^{-1}$  at both 1665 and 1667 MHz are suggestive of Zeeman splitting in a magnetic field of  $\sim 1.3 \text{ mG}$  ( $1 \text{ mG} \equiv 10^{-7} \text{ T}$ ). Weak excited state (6035 MHz) OH emission was discovered by Knowles *et al.* (1976).

OH 301.14–0.23 (Fig. 3). This is a new OH maser with strong emission in the velocity range  $-37$  to  $-41 \text{ km s}^{-1}$ . At  $v = -50 \text{ km s}^{-1}$  weaker emission occurs at both 1665 and 1667 MHz; the oppositely polarised pairs of features suggest Zeeman splitting in a magnetic field of  $1.7 \text{ mG}$ . A feature at still higher velocity,  $v = -64 \text{ km s}^{-1}$ , is present on the 1665 MHz transition. The associated  $\text{H}_2\text{O}$  maser has emission near both  $-40 \text{ km s}^{-1}$  and at these displaced velocities. The continuum source in this direction is weak and has not been searched for recombination-line emission; however, it seems most likely that the systemic velocity is  $\sim -40 \text{ km s}^{-1}$ , and the displaced features seen on the  $\text{H}_2\text{O}$  spectrum are typical of the 'high-velocity features' seen in other  $\text{H}_2\text{O}$  masers. Despite the occurrence of such features in about 5% of all  $\text{H}_2\text{O}$  masers, previous searches for 'high-velocity' OH counterparts have been in vain, OH 301.14–0.23 being the first to show such emission. The displacements for both OH and  $\text{H}_2\text{O}$  are similar if measured in velocity (rather than frequency), and this confirms that the displacements are *kinematic* rather than due to more exotic *scattering* mechanisms, since the latter would be expected to cause displacements similar in *frequency* for the OH and the  $\text{H}_2\text{O}$  masers.

OH 305.20+0.21 (Fig. 4). First reported by Caswell *et al.* (1977); there has been very little variation since 1976. Note confusion with the following two sources; despite this confusion, it appears that at least some of the 1667 MHz emission comes from this position.

OH 305.21+0.03 (Fig. 4). Note the proximity of this new source to the preceding and following sources; on the profile shown, only the LH feature with  $v = -34 \text{ km s}^{-1}$  is from this position.

OH 305.36+0.15 (Fig. 4). Originally reported by Goss *et al.* (1970). Since the discovery measurement, the 1665 MHz features between  $v = -33$  and  $-38 \text{ km s}^{-1}$  have weakened to half their original intensity but the feature at  $v = -39.5 \text{ km s}^{-1}$  has increased by a factor of two.

OH 305.81–0.24 (Fig. 2). A new OH maser with a very strong associated  $\text{H}_2\text{O}$  maser. The oppositely polarised pairs of OH features at both 1665 and 1667 MHz are suggestive of Zeeman splitting in a field of  $2.7 \text{ mG}$ .

OH 306.32–0.36 (no figure). In June 1980 we detected this source at 1665 MHz with intensity  $\sim 2 \text{ Jy}$  in LH polarisation at a velocity of  $-23 \text{ km s}^{-1}$ . The associated

compact HII region has a velocity of  $-16 \text{ km s}^{-1}$  and there is formaldehyde absorption at  $-19 \text{ km s}^{-1}$ . In February 1982 OH emission was barely discernible and no position measurement was possible. We conclude that the OH maser showed significant intensity variations over the 20-month interval, and list its position as that of the radio HII region. Since we see no optical counterpart to the radio HII region, we adopt the far distance of  $10.7 \text{ kpc}$  as more likely than the near distance of  $1.2 \text{ kpc}$ . No  $\text{H}_2\text{O}$  maser was detected in the immediate vicinity of this position,  $\pm 50''$  arc, which indicates either that the OH maser position is displaced from the continuum peak by as much as  $2'$  arc, or that there is no strong  $\text{H}_2\text{O}$  counterpart.

*OH 308.92+0.12* (Fig. 5). This maser was first observed by Robinson *et al.* (1974). At 1665 MHz the appearance has now changed completely. At 1667 MHz the appearance has remained similar, but with the dominant feature now reduced to  $\sim \frac{1}{2}$  intensity. An  $\text{H}_2\text{O}$  maser is associated, and the masers coincide with a compact HII region with flux density  $0.4 \text{ Jy}$ , as seen on the  $1.4 \text{ GHz}$  synthesis map of the region (Caswell *et al.* 1981). The continuum source position R.A.  $13^{\text{h}}39^{\text{m}}34^{\text{s}}.3$ , Dec.  $-61^{\circ}53'49''$  has an r.m.s. uncertainty of  $2''$  arc and is probably the most accurate estimate of the maser positions. Epchtein *et al.* (1981) detected IR emission which probably arises from the cool dust associated with the compact HII region.

*OH 309.92+0.48* (Fig. 5). First observed by Robinson *et al.* (1974). At 1665 MHz the three major features are still present, one with unchanged intensity, one increased and one decreased. At 1667 MHz the two features have remained unchanged (to within 20%). An early report of an  $\text{H}_2\text{O}$  maser (Kaufmann *et al.* 1977) has recently been confirmed in our unpublished Parkes observations. An HII region with  $v = -55 \text{ km s}^{-1}$  has an extension suggestive of a weak compact component (Haynes *et al.* 1978) at the position of the OH maser. An IR source detected by Epchtein *et al.* (1981) at R.A.  $13^{\text{h}}47^{\text{m}}12^{\text{s}}.7$ , Dec.  $-61^{\circ}20'17'' \pm 5''$  probably arises from the compact source. The OH maser is notable for its intense excited state (6035 MHz) emission, discovered by Knowles *et al.* (1976).

*OH 310.06-3.02* (Fig. 6). This new OH maser was detected by accident at what was intended to be a reference position displaced from the galactic plane. It has an associated  $\text{H}_2\text{O}$  maser. An IR source in this direction is listed in the IRAS point source catalogue (Beichman *et al.* 1985) and has colours indicative of the warm dust shell around a late-type star rather than the cooler dust of an HII region; furthermore, no optical nebula is visible on the Southern Sky Atlas SRC(J) film of the region. Identification with the expanding shell of a late-type star is also predicated by the wide velocity spread of the 1665 MHz OH emission, corresponding to a shell expansion velocity of  $\sim 10 \text{ km s}^{-1}$ . In such sources 1612 MHz emission is commonly stronger than main-line emission in the outer shell (the outer extremities of the velocity range). In OH 310.06-3.02 we find indeed that 1612 MHz emission is present (P.te Lintel, H. J. Habing, J. L. Caswell, R. F. Haynes and R. P. Norris, unpublished data), but surprisingly it is confined between velocities  $-4$  and  $0 \text{ km s}^{-1}$ , near the centre of the range seen at 1665 MHz. Furthermore, the emission at 1665 MHz is stronger than at 1667 MHz, contrary to the usual situation in late-type stars. Conditions of excitation are clearly unusual, and this strange source merits much more detailed study.

*OH 311.64-0.38* (Fig. 6). This new maser is intense on both 1665 and 1667 MHz transitions and has a mean (systemic) velocity of  $+34 \text{ km s}^{-1}$ . This positive velocity indicates that it lies outside the solar circle, at an unambiguous distance of  $16.3 \text{ kpc}$ .

It thus helps to delineate a distant portion of the Carina arm. An  $\text{H}_2\text{O}$  maser coincides with the OH maser and has a similar mean velocity. The continuum emission is weak but is probably part of an HII complex whose peak at  $311.11-0.27$  has a recombination-line velocity of  $+36 \text{ km s}^{-1}$  (Caswell and Haynes 1986).

*OH 311.94+0.14 (Fig. 7).* This weak new OH maser lies in the direction of an intense  $\text{H}_2\text{O}$  maser first reported by Braz and Scalise (1982). The OH maser was not detectable at any offset positions and thus the position is poorly determined; we quote the position which we measured for the  $\text{H}_2\text{O}$  maser. There is prominent OH absorption here (see Fig. 7), probably arising from two absorbing clouds with velocities of  $-50$  and  $-44 \text{ km s}^{-1}$ . The maser is in the direction of the edge of an HII region with recombination-line velocity of  $-47 \text{ km s}^{-1}$ , and a separate nearby HII region has a velocity of  $-45 \text{ km s}^{-1}$ . Caswell *et al.* (1975) reported HI absorption measurements which indicate that both HII regions,  $G311.9+0.1$  and  $G311.9+0.2$ , lie at the far kinematic distance,  $\sim 9.8 \text{ kpc}$ .

*OH 313.47+0.19 (Fig. 7).* A new OH maser coinciding with a compact HII region with velocity  $-5 \text{ km s}^{-1}$ . The absence of optical emission suggests that the HII region (and the presumably associated OH maser) is probably at the far distance of  $13.4 \text{ kpc}$  rather than the near distance of  $0.3 \text{ kpc}$ .

*OH 316.40-0.30 (Fig. 7).* This weak new OH maser lies at the edge of a compact HII region. The HII region velocity is  $+3 \text{ km s}^{-1}$ . Possible kinematic distances are  $\sim 0$  and  $14.7 \text{ kpc}$ ; we adopt the latter, since no optical counterpart is visible.

*OH 316.64-0.08 (Fig. 8).* The OH maser was first detected by Caswell *et al.* (1977); an  $\text{H}_2\text{O}$  maser has not been detected at this position (CBFW 87). Extended continuum emission is present in this general direction, with the strongest feature,  $G316.8-0.1$ , showing a recombination-line velocity of  $-36 \text{ km s}^{-1}$ ; however, some nearby sources have considerably different velocities of  $+3 \text{ km s}^{-1}$  (see notes on the previous source) and  $-49 \text{ km s}^{-1}$ . There has been some argument as to the distance of  $G316.8-0.1$ —whether it lies at the near ( $2.6 \text{ kpc}$ ) or far ( $11.8 \text{ kpc}$ ) kinematic distance (Shaver *et al.* 1981). The mean velocity of the maser OH 316.64-0.08 is  $v = -22 \text{ km s}^{-1}$  and it lies near the most prominent optical emission. The latter probably represents an HII region distinct from  $G316.8-0.1$  and its optical prominence suggests it is at the near distance corresponding to  $v = -22 \text{ km s}^{-1}$ , i.e.  $1.5 \text{ kpc}$ , rather than at the far distance of  $13 \text{ kpc}$ .

*OH 316.76-0.02 (Fig. 8).* This OH maser was discovered by Haynes *et al.* (1976) (see also Caswell *et al.* 1977), and is coincident with an  $\text{H}_2\text{O}$  maser. The high-resolution continuum map (at  $1.4 \text{ GHz}$ ) and the red photograph reproduced by Shaver *et al.* (1981) show that these masers are slightly displaced from the HII region. The maser velocities ( $\sim -39 \text{ km s}^{-1}$ ), the OH absorption velocity (centred near  $-38 \text{ km s}^{-1}$ ), and the recombination-line velocity ( $-36 \text{ km s}^{-1}$ ) are all similar and correspond to a near kinematic distance of  $2.6 \text{ kpc}$ . The OH maser has changed considerably since the earlier observations of Caswell *et al.* (1977).

*OH 316.81-0.07 (Fig. 8).* A new OH maser in close positional agreement with a known  $\text{H}_2\text{O}$  maser (Batchelor *et al.* 1980) and the peak of a strong, compact, continuum radio source (Shaver *et al.* 1981); an IR source, designated IRS10 by Shaver *et al.*, is also at this position.

*OH 318.05+0.08 (Fig. 8).* This is a new OH maser, and a newly discovered  $\text{H}_2\text{O}$  maser coincides with it. Both masers are strong and have velocities centred near  $v = -53 \text{ km s}^{-1}$ ; the corresponding kinematic distances are  $3.7$  and  $11.1 \text{ kpc}$ . A

weak argument favouring the nearer distance is that the OH maser would be amongst the strongest sources known if it were at the far distance. The radio continuum emission is extended and very weak.

*OH 318.95–0.20 (Fig. 9).* A weak new maser with mean velocity  $-36 \text{ km s}^{-1}$ . In approximately the same direction is an  $\text{H}_2\text{O}$  maser with mean velocity  $-32 \text{ km s}^{-1}$  and a compact radio HII region with  $v = -29 \text{ km s}^{-1}$ . The 1665 MHz OH maser emission has varied rapidly, weakening by a factor of three between 1981 September and 1982 February.

*OH 319.39–0.02 (Fig. 9).* The intensities of this weak new OH maser are comparable at 1665 and 1667 MHz. It coincides with a radio continuum HII region. The OH maser is one of the two in our survey where no corresponding  $\text{H}_2\text{O}$  source has been found.

*OH 320.23–0.28 (Fig. 9).* The OH maser was first discovered by Robinson *et al.* (1974). At 1665 and 1667 MHz all features seen at one epoch can be seen at the other epoch (a decade apart); the largest intensity variation is a 2.5 times increase in the RH feature with  $v = -67.6 \text{ km s}^{-1}$ . Scalise and Braz (1980) reported an  $\text{H}_2\text{O}$  maser in this direction which has recently been confirmed at Parkes. A compact HII region is also present.

*OH 324.20+0.12 (Fig. 11).* Discovered by Robinson *et al.* (1974); the features now seen, a decade later, remain similar, apart from variations of intensity of up to 50%. An  $\text{H}_2\text{O}$  maser is also present; our new estimate of the OH position is close to that of the  $\text{H}_2\text{O}$  maser (coincident to within the uncertainties), the mean of OH and  $\text{H}_2\text{O}$  positions being R.A.  $15^{\text{h}}29^{\text{m}}01^{\text{s}}.5$ , Dec.  $-55^{\circ}46'01''$ . This position is towards the edge of a fairly compact HII region. Epchtein and Lepine (1981) found an IR steep-spectrum (i.e. cool) source at R.A.  $15^{\text{h}}29^{\text{m}}01^{\text{s}}.9$ , Dec.  $-55^{\circ}46'09''$  which essentially coincides with the maser positions (their remark that the OH maser is displaced was based on the earlier and less accurate measurement by Robinson *et al.* 1974). The high systemic velocity indicates that the maser/HII region complex must be quite distant, and approximately at the tangential point (8.1 kpc away).

### (c) Null Results of Special Interest

The directions where no OH maser emission was seen above our detection limits included a number of  $\text{H}_2\text{O}$  maser positions and these null results are of particular interest.

*G264.29+1.47.* In the direction of this HII region (known optically as RCW 34), there is a prominent  $\text{H}_2\text{O}$  maser (Braz and Scalise 1982; and our unpublished Parkes data, CBFW 87). No 1665 MHz OH maser was detectable in June 1980.

*G265.14+1.45.* Strong HII region (RCW 36) with weak  $\text{H}_2\text{O}$  maser (Braz and Scalise 1982; CBFW 87); no 1665 MHz OH maser detectable in June 1980, but OH absorption is prominent (Caswell and Robinson 1974). Weak emission in this direction was reported by Turner (1979), using an  $18'$  arc beam: if it is a maser its accurate position is unknown, since no surrounding positions were observed; alternatively, reduced absorption over a small velocity range would satisfactorily fit Turner's spectrum, since it does not rise above the zero level and no polarisation data were obtained.

*G267.94–1.06.* Strong HII region (RCW 38) with prominent  $\text{H}_2\text{O}$  maser (Batchelor *et al.* 1980); OH absorption but no emission—as noted by Caswell *et al.* (1977).

*G269.16-1.13.* Strong HII region (RCW 39) with H<sub>2</sub>O maser (Scalise and Braz 1980; CBFW 87); OH absorption is present and weak 1665 MHz emission (0.4 Jy) embedded in the absorption was found at a marginally significant level in September 1977 but was not detectable in September 1981.

*G270.26+0.83.* A weak HII region with strong H<sub>2</sub>O maser (Scalise and Braz 1980; CBFW 87). No OH maser detected in February 1982.

*G284.36-0.42.* An intense H<sub>2</sub>O maser (Scalise and Schaal 1977; Batchelor *et al.* 1980) lies in the direction of this strong HII region, RCW 49. The continuum emission raises the system temperature and leads to poorer sensitivity for any OH search in this direction. A possible OH detection was made (0.9 Jy,  $v = +8 \text{ km s}^{-1}$  in the RH sense of polarisation at 1665 MHz in February 1982), but is of marginal significance, near the  $3\sigma$  level.

*G287.37-0.62.* An H<sub>2</sub>O maser is present here (Scalise and Braz 1980; CBFW 87), near the peak of the Carina nebula HII region. OH absorption is present near  $v = -24 \text{ km s}^{-1}$ , but no emission was detectable at 1665 MHz in February 1982; the upper limit of  $\sim 1 \text{ Jy}$  is poor owing to the strong continuum emission.

*G291.27-0.71.* An H<sub>2</sub>O maser is present (e.g. Batchelor *et al.* 1980) towards this strong HII region, but no 1665 MHz maser emission is detectable (Caswell *et al.* 1977).

*G298.21-0.33.* Strong HII region, with weak H<sub>2</sub>O maser (Braz and Scalise 1982; CBFW 87); 1665 MHz observations in October 1980 showed weak absorption near  $v = +30 \text{ km s}^{-1}$  but no emission.

### 3. Discussion

#### (a) Galactic Distribution and Luminosity Function of Type I OH Masers

In Part II we derived a preliminary galactic distribution and luminosity function based on the 85 masers between longitude  $326^\circ$  and the galactic centre. The addition of the present 35 sources increases the total sample to 120 masers and permits improved estimates of both distributions. The region of galactic disc searched has been increased and thus the correction factors needed to allow for incomplete searching are reduced and correspondingly more reliable.

We have proceeded in the manner which we described in detail in Part II. Fortunately only 10 of the additional 35 sources have unresolved ambiguities in their kinematic distances and for statistical purposes these have been assigned in equal numbers to the near and far alternative distances according to the criteria of Part II (in general the apparently weaker sources are assumed to be further away).

The resulting distribution is shown in Fig. 12.

*Radial Distribution.* As was the case for our earlier surveys, the limiting sensitivity is  $S \approx 1 \text{ Jy}$ . We wish to derive a radial distribution estimate for a sample complete to a limiting luminosity,  $Sd^2$ . Consideration was restricted to sources with luminosity  $> 100 \text{ Jy kpc}^2$  so as to include the galactic centre in the region to which we were fully sensitive. (The Sun is assumed to lie 10 kpc from the galactic centre.) The sources were binned in galactocentric annuli of width 1 kpc, and, before summing, a weight was applied to each source, depending on its luminosity, in order to correct for the limited fraction of the annulus which had been effectively searched. The weight is simply a factor of 2 for strong sources within the solar circle (to allow for searching

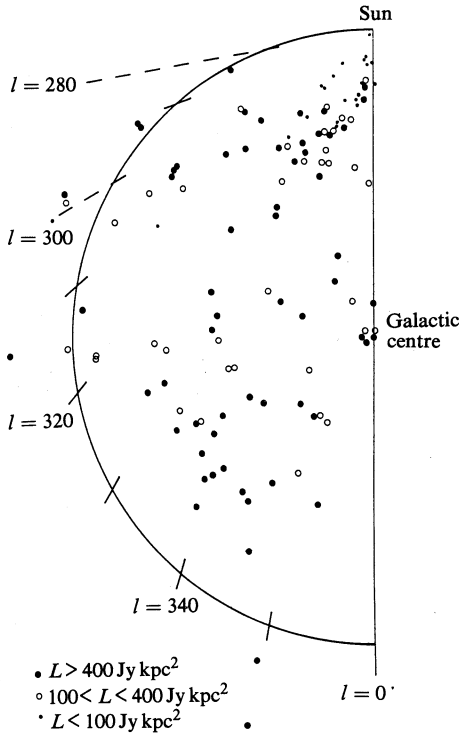


**Fig. 12.** Distribution of 1665 MHz (Type I) OH masers, showing the 120 sources from the present survey and Parts I and II from galactic longitude 270° through 360° to 2°. See Section 3a for a discussion of the assignment of distances.

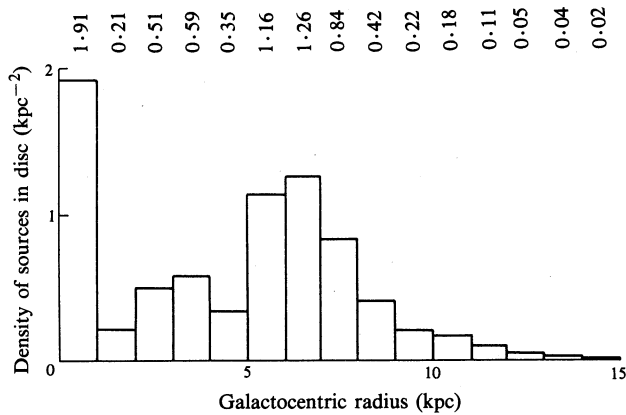


**Fig. 13.** Histogram showing the spatial density of Type I OH masers in the galactic disc as a function of galactocentric radius. (The Sun is assumed to be 10 kpc from the galactic centre.) Histogram values are written above each bar.

only half the Galaxy) and reaches a worst-case value of  $\sim 5$  for some of the weakest ones. For comparison we note that weighting factors as high as 50 were necessary in Part II owing to the small fraction of the outer galaxy that had been surveyed.

The resulting radial distribution is shown in Fig. 13. The sources added from the present survey all lie at  $R > 5$  kpc and greatly improve our assessment of the

distribution at these larger radii. Qualitatively it can be seen that the distribution falls off only slowly at large  $R$ , in agreement with our earlier tentative conclusion. The maximum of the distribution again lies between 6 and 7 kpc, although less strongly peaked than previously estimated. Overall we now find that 207 masers are present with  $L > 100 \text{ Jy kpc}^2$  within the solar circle. (This may be compared with our earlier estimates in Part II of 312 or 329—with large uncertainties caused by the higher weighting factors needed to allow for incompleteness.) Outside the solar circle lie an additional  $\sim 30$  masers (about 12% of the total), and their distribution is shown with statistical fluctuations smoothed.

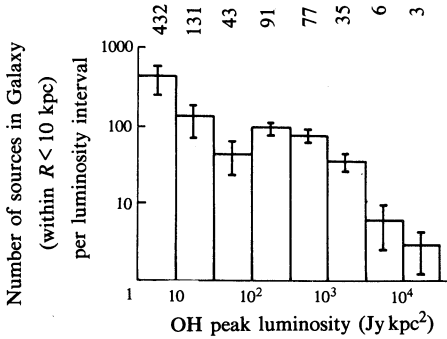


Fig. 14. Luminosity function for OH masers at 1665 MHz normalised to the total expected in the galactic disc out to the solar distance (assumed to be 10 kpc). The error bars allow only for statistical errors, i.e. proportional to  $n^{1/2}$ , where  $n$  is the observed (uncorrected) number of sources in each bin. Histogram values are written above each bar.

**Luminosity Function.** The luminosity function, derived in the same way as in Part II, is shown in Fig. 14 and is normalised to the total expected in the galactic disc out to the solar distance. It is in fair agreement with our earlier estimate but with systematically lower numbers, indicating that our previous correction factors were slightly overestimated. As in Part II, the source numbers increase with decreasing luminosity, at least down to  $L = 100 \text{ Jy kpc}^2$ ; at lower luminosities statistical errors make the trend uncertain, and furthermore the weighting factors needed to correct for limited sensitivity are much larger and less reliable than at higher luminosity. Nonetheless, the trend for the numbers of masers to continue to increase with decreasing luminosity appears to hold down to the  $3 \text{ Jy kpc}^2$  limit of the plotted distribution; this is in spite of a bias in the opposite direction which we introduced by assigning the apparently weakest sources to far (rather than near) distances when there was an ambiguity. Our estimate of 818 masers having  $Sd^2 > 3 \text{ Jy kpc}^2$  within the solar circle ( $R < 10 \text{ kpc}$ ) would increase to  $\sim 930$  in the whole Galaxy if  $\sim 12\%$  of the maser population lies at  $R > 10 \text{ kpc}$  (assuming the same spatial distribution as derived for the more luminous sources, with  $Sd^2 > 100 \text{ Jy kpc}^2$ ).

#### (b) Relative Intensities of the Four Ground-state Transitions

In 32 of the 35 masers in our present survey the 1665 MHz transition shows stronger emission than the 1667 MHz transition; overall, 107 out of the 120 masers in our total sample are most intense at 1665 MHz.

In our present survey satellite line data are available only for 10 sources; apart from the peculiar maser OH 310.06–3.02, none of these show emission on the satellite lines, a statistic compatible with the 1-in-6 fraction found in Part II.

(c) *Velocity Structure and Polarisation*

One source, OH 301.14–0.23 (Fig. 3), shows emission displaced in velocity by  $20 \text{ km s}^{-1}$  from the main features and closely resembles its associated  $\text{H}_2\text{O}$  maser in this respect (CBFW 87); while such high-velocity features are common amongst  $\text{H}_2\text{O}$  masers, this is the first clear-cut example where corresponding features have been detected in OH.

The 1667 MHz emission of OH 301.14–0.23 shows a pair of features with opposite senses of circular polarisation near  $v = -51 \text{ km s}^{-1}$  which may be accounted for by Zeeman splitting. Two other sources, OH 300.97+1.15 and OH 305.81–0.24, also show polarisation and velocity structure consistent with Zeeman splitting, as discussed in the notes of Section 2*b*.

(d) *Association of  $\text{H}_2\text{O}$  Masers*

As we have noted in column 11 of Table 1,  $\text{H}_2\text{O}$  masers have been detected in the direction of 33 of the 35 OH masers; furthermore, one of the remaining two OH masers has an uncertain position, which implies that the  $\text{H}_2\text{O}$  null result may not be significant. The detection rate of associated  $\text{H}_2\text{O}$  masers is thus remarkably high. The  $\text{H}_2\text{O}$  results will be discussed in detail elsewhere (CBFW 87).

(e) *Association with IR Sources*

In the notes of Section 2*b* we referenced earlier discussions of IR sources likely to be associated with several of the OH masers. Subsequently our checks of the recent point source catalogue of the IRAS survey (Beichman *et al.* 1985) reveal that all the masers have strong IR sources nearby (although in a few cases an HII region complex is so bright and extended that identification with a specific compact component is not possible). Except for OH 310.06–3.02 all these IR sources are more intense at  $60 \mu\text{m}$  than at  $25 \mu\text{m}$  by at least a factor of 4 and represent a cocoon of cool dust associated with HII regions. These associations will be considered further in conjunction with our  $\text{H}_2\text{O}$  data in a future paper (CBFW 87).

#### 4. Conclusions

With the completion of the present survey nearly half of the galactic disc within the solar circle has been searched for main-line OH maser emission down to a uniform sensitivity limit. The radial distribution derived from the survey shows a broad maximum near  $R = 6.5 \text{ kpc}$  similar to the location of maximum CO emission in the southern sky (McCutcheon *et al.* 1981). Both CO and the OH masers trace regions of star formation. Consequently it would be valuable to extend the OH survey with similar sensitivity to the complementary sector of the Galaxy,  $l = 0^\circ \rightarrow 90^\circ$ , since, as we noted in Part II, the radial distributions of CO emission and HII regions at  $l > 0^\circ$  differ from the southern distribution in so far as the maximum is displaced by  $\sim 1 \text{ kpc}$  to smaller values of  $R$ . Such a displacement is hardly unexpected if the objects lie in spiral arms with a non-negligible pitch angle.

Now that the global properties of the large sample of OH masers have been well established we are selecting some of these objects for study in depth, in an attempt to relate the OH masers to associated compact HII regions, IR sources and  $\text{H}_2\text{O}$  masers (Forster and Caswell 1987).

## References

- Batchelor, R. A., Caswell, J. L., Goss, W. M., Haynes, R. F., Knowles, S. H., and Wellington, K. J. (1980). *Aust. J. Phys.* **33**, 139.
- Beichman, C. A., Neugebauer, G., Habing, H. J., Clegg, P. E., and Chester, T. J. (Eds) (1985). 'IRAS Catalogs and Atlases—Explanatory Supplement' (US Govt Printing Office: Washington, DC).
- Braz, M. A., and Scalise, E. (1982). *Astron. Astrophys.* **107**, 272.
- Caswell, J. L., Batchelor, R. A., Forster, J. R., and Wellington, K. J. (1987). *Aust. J. Phys.* (to be submitted).
- Caswell, J. L., and Haynes, R. F. (1983). *Aust. J. Phys.* **36**, 361.
- Caswell, J. L., and Haynes, R. F. (1986). *Astron. Astrophys.* (in press).
- Caswell, J. L., Haynes, R. F., and Goss, W. M. (1977). *Mon. Not. R. Astron. Soc.* **181**, 427.
- Caswell, J. L., Haynes, R. F., and Goss, W. M. (1980). *Aust. J. Phys.* **33**, 639.
- Caswell, J. L., Milne, D. K., and Wellington, K. J. (1981). *Mon. Not. R. Astron. Soc.* **195**, 89.
- Caswell, J. L., Murray, J. D., Roger, R. S., Cole, D. J., and Cooke, D. J. (1975). *Astron. Astrophys.* **45**, 239.
- Caswell, J. L., and Robinson, B. J. (1974). *Aust. J. Phys.* **27**, 597.
- Epchtein, N., Guibert, J., Rieu, N.-Q., Turan, P., and Wamsteker, W. (1981). *Astron. Astrophys.* **97**, 1.
- Epchtein, N., and Lepine, J. R. D. (1981). *Astron. Astrophys.* **99**, 210.
- Forster, J. R., and Caswell, J. L. (1987). In 'Star Forming Regions', Proc. IAU Symp. No. 115 (Reidel: Dordrecht) (in press).
- Frogel, J. A., and Persson, S. E. (1974). *Astrophys. J.* **192**, 351.
- Frogel, J. A., Persson, S. E., and Aaronson, M. A. (1977). *Astrophys. J.* **213**, 723.
- Goss, W. M., Manchester, R. N., and Robinson, B. J. (1970). *Aust. J. Phys.* **23**, 559.
- Goss, W. M., Radhakrishnan, V., Brooks, J. W., and Murray, J. D. (1972). *Astrophys. J. Suppl. Ser.* **24**, 123.
- Haynes, R. F., Caswell, J. L., and Goss, W. M. (1976). *Proc. Astron. Soc. Aust.* **3**, 57.
- Haynes, R. F., Caswell, J. L., and Simons, L. W. J. (1978). *Aust. J. Phys. Astrophys. Suppl.* No. **45**, 1.
- Kaufmann, P., Zisk, S., Scalise, E., Schaal, R. E., and Gammon, R. H. (1977). *Astron. J.* **82**, 577.
- Knowles, S. H., Caswell, J. L., and Goss, W. M. (1976). *Mon. Not. R. Astron. Soc.* **175**, 537.
- McCutcheon, W. H., Robinson, B. J., and Whiteoak, J. B. (1981). *Proc. Astron. Soc. Aust.* **4**, 243.
- Manchester, R. N., Robinson, B. J., and Goss, W. M. (1970). *Aust. J. Phys.* **23**, 751.
- Retallack, D. S., and Goss, W. M. (1980). *Mon. Not. R. Astron. Soc.* **193**, 261.
- Robinson, B. J., Caswell, J. L., and Goss, W. M. (1974). *Aust. J. Phys.* **27**, 575.
- Scalise, E., and Braz, M. A. (1980). *Astron. Astrophys.* **85**, 149.
- Scalise, E., and Schaal, R. E. (1977). *Astron. Astrophys.* **57**, 475.
- Schmidt, M. (1965). In 'Galactic Structure' (Eds A. Blaauw and M. Schmidt), p. 513 (Univ. Chicago Press).
- Shaver, P. A., Retallack, D. S., Wamsteker, W., and Danks, A. C. (1981). *Astron. Astrophys.* **102**, 225.
- Turner, B. E. (1979). *Astron. Astrophys. Suppl. Ser.* **37**, 1.